AIAA JOURNAL
Vol. 34, No. 11, November 1996

Inverse Aeroacoustic Problem for a Streamlined Body Part 2: Accuracy of Solutions

Sheryl Patrick Grace* and Hafiz M. Atassi†
University of Notre Dame, Notre Dame, Indiana 46556
and
William K. Blake‡
David Taylor Model Basin, Bethesda, Maryland 20084-5000

Previously established methods for performing the aeroacoustic inversion for a flat-plate airfoil are tested to determine their sensitivity to errors in both the far-field input data and the mean-flow input parameters. The results of the sensitivity analysis for the input data show that the magnification of input error due to ill-posedness can be controlled by optimal choices of the regularization parameter and the input data locations. A similar sensitivity analysis of the effect of mean-flow parameters—Mach number and reduced frequency—shows strong dependence of the inverse process on these parameters. In this case, improvements in the reconstructions can be obtained by using input data from the midfield.

Introduction

In Part 1 of this paper, we established the feasibility of the inverse aeroacoustic problem for a streamlined body using "perfect" input data.[1] The "perfect" input data are generated by solving the direct problem using known semianalytical solutions.[2] These solutions are obtained by solving Possio's integral equation for the pressure jump along a flat-plate airfoil in response to a three-dimensional gust. Equation (5) of Part 1 (Ref. 1) then is used to calculate the linearized prediction for the radiated sound.

In application, the far-field data will be obtained experimentally. Therefore, the data will contain noise from the surroundings, as well as nonlinear effects inherent to the acoustic propagation. Also, it will have an associated measurement uncertainty attributable to the mechanical and electrical systems used to acquire the data. Thus, although the inversion is feasible, to be useful in practice, it must be robust when the input is not "perfect." Hence, in this paper, the schemes that give good results for "perfect" input data are reexamined for their accuracy when the input data contain noise.

In Part 1, we developed three methods for the inversion with "perfect" input data. The first such method uses 1) an asymptotic form of the kernel along with the transformation $y_1 = -\cos\gamma$, 2) a simple quadrature method for the discretization of the integral equation, and 3) Tikhonov regularization. This method was denoted as the expanded kernel method. The other two methods use collocation to transform the integral equation into a matrix equation. These two methods are very similar except for the form of the kernel in the integral equation; one uses the full kernel whereas the other uses a far-field expansion of the kernel. In both methods, an a priori cutoff regularization, similar to the spectral cutoff, is used.

Here, we examine the inherent sensitivity of the inverse solutions to noise in the input data and show that this sensitivity can be controlled by an optimal choice of the regularization scheme and the associated parameter. Moreover, one expects that the mean-flow input parameters—Mach number and reduced frequency—also may have errors associated with them. The sensitivity to this type of error cannot be handled within the singular value decomposition (SVD) method because it directly affects the kernel of the integral equation, which in turn affects the matrix. However, because errors associated with inaccurate input parameters result from large variations of phase of the far-field pressure, it is shown that this sensitivity can be reduced by using input data from the midfield.

Received Sept. 1, 1995; revision received May 20, 1996; accepted for publication May 27, 1996; also published in *AIAA Journal on Disc*, Volume 1, Number 4.

*Research Assistant, Aerospace and Mechanical Engineering Department; currently Assistant Professor, Aerospace and Mechanical Engineering Department, Boston University, 110 Cummington Street, Boston, MA 02215. Member AIAA.

†Professor, Aerospace and Mechanical Engineering Department. Associate Fellow AIAA.

‡Chief Scientist, Hydroacoustics, C.D. Code 7023, N.S.W.C. Building 3, Room 221.

Sensitivity Study

It has already been stated that the ill-posedness of the inverse aeroacoustic problem implies that small errors in the input data will be magnified in the solution. To demonstrate this, we choose a case presented in Part 1 for which we found a very accurate inversion when using "perfect" input data. The case under consideration corresponds to $M = 0.4$ and $k_1 = 5.0$. The inversion method we consider first uses the quadrature method for forming the matrix, the Tikhonov regularization scheme within the SVD and a regularization parameter, $\alpha = 10^{-4}$. Now, instead of using our "perfect" input

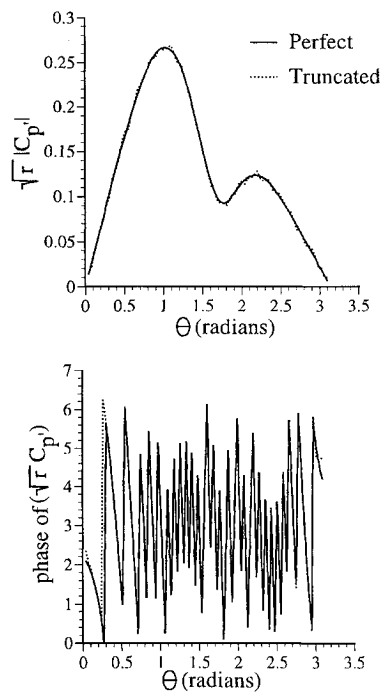

Fig. 1 Magnitude (top) and phase (bottom) of the truncated input data ($M = 0.4, k_1 = 5.0$).

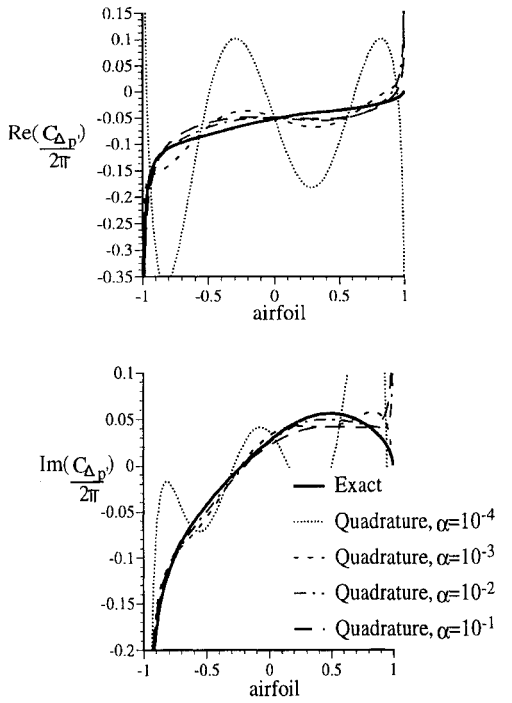

Fig. 2 Effect of varying the Tikhonov regularization parameter when using truncated input data: real (top) and imaginary (bottom) parts of the unsteady surface pressure ($M = 0.4, k_1 = 5.0$).

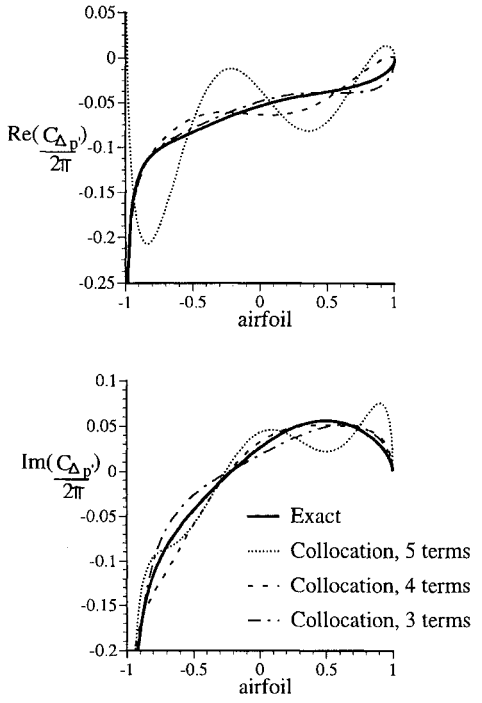

Fig. 3 Effect of varying the a priori cutoff value with the collocation technique when using truncated input data: real (top) and imaginary (bottom) parts of the unsteady surface pressure ($M = 0.4, k_1 = 5.0$).

data, we perturb the data slightly by simply truncating the data while allowing rounding. The truncated data are represented by the dotted line in Fig. 1, and the deviation is barely noticeable. Inputing these slightly perturbed data into the inversion scheme, we arrive at a wildly oscillating reconstruction. The reconstruction of the unsteady pressure using this input data and $\alpha = 10^{-4}$ is shown by the dotted line in Fig. 2. As in Part 1, the figures representing the reconstructions contain plots of both the real and the imaginary parts of the nondimensional unsteady pressure jump along the flat-plate airfoil, and the thick solid line represents the "perfect" reconstruction.

It is easy to see how this inherent magnification of error is produced in our solution scheme. The solution to the matrix equation,

$$[A] = [\mathcal{M}][B] \tag{1}$$

is constructed through the SVD as follows:

$$[B] = \sum_i \frac{[A] \cdot [u_i]}{\sigma_i} [v_i] \tag{2}$$

Hence, any errors in the input A will be magnified when dividing by small singular values. Although the Tikhonov regularization scheme is intended to damp out the influence of small singular values by modifying the denominator in Eq. (2) to the quantity $(\sigma_i^2 + \alpha)/\sigma_i$, apparently the damping was not strong enough. It follows, then, that the oscillations in the reconstruction shown in the preceding example can possibly be controlled by increasing the regularization parameter.

The results obtained when the regularization parameter in the preceding example is increased to 10^{-3}, 10^{-2}, and finally 10^{-1} are shown in Fig. 2. As the parameter increases, the reconstructions improve significantly. The best choice of the regularization parameter for the Tikhonov regularization scheme is not well defined a priori, and currently it is set through calibration.

The method of reconstruction, denoted in Part 1 as the collocation method, is more easily adapted to handle input errors because it uses a cutoff regularization. In the cutoff regularization, only the singular values and the related singular vectors above the cutoff are used in the reconstruction. From Eq. (2), we see that any singular value below 1.0 can magnify errors in the input vector A. Hence, when the input data contain noise, it is best to set the cutoff parameter to 1.0. We illustrate this in the following example.

When the input data were "perfect," the a priori cutoff value was 0.01 for the singular values. Using this cutoff value with the truncated input data gives the inaccurate reconstruction shown as the dotted line in Fig. 3. Reducing the number of columns such that the smallest singular value is 1.0 gives a much more accurate reconstruction, as shown by the dash-dot-dash line in Fig. 3. The only difference between the reconstructions shown in Fig. 3 is the number of terms used in the collocation series. A five-term collocation series coincides with a cutoff parameter of 0.01 and leads to an inadequate reconstruction. A three-term collocation series coincides with a cutoff parameter of 1.0 and yields a much better reconstruction. We note that setting the a priori cutoff parameter to 1.0 greatly reduces the sensitivity to errors in the input data while still allowing for satisfactory results when "perfect" input data are used; however, it precludes obtaining a "perfect" reconstruction when "perfect" input data are used.

Truncating the data has demonstrated the ill-posedness of the inverse aeroacoustic problem and has defined the new regularization parameters. However, a more realistic study of the sensitivity of the inverse solutions to the far-field data is required. To this end, it is assumed that k_1 and M are known accurately. Several methods for perturbing the input data are used, and the corresponding reconstructions are shown. The reconstructions are obtained using both the quadrature method, with expanded kernel and $y_1 = \cos\gamma$ transformation, as well as the collocation method with expanded kernel. The combination of $M = 0.4$ and $k_1 = 5.0$ is studied for each error type. For every type of error, both the "perfect" input data and the noisy input data are plotted, as well as their respective reconstructions.

Relative Error

The first type of error considered is a relative error. The magnitude and phase of the far-field data are both perturbed by ±20% at every simulated measurement location. In Fig. 4, the solid line represents the "perfect" input data, and the dotted line shows the imperfect input data for the case $M = 0.4$, $k_1 = 5.0$. Both the magnitude and the phase of the input are included. The reconstructions obtained from the quadrature and collocation methods are shown in Fig. 5. The results are not "perfect" for either scheme. However, when one considers the large amount of error introduced in the input data, both reconstructions seem satisfactory.

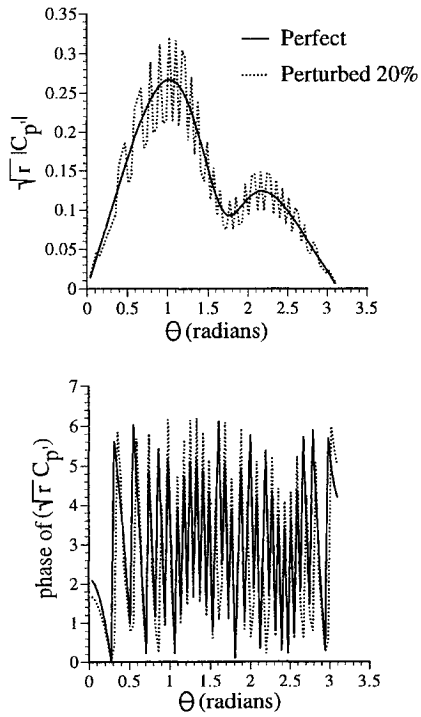

Fig. 4 Magnitude (top) and phase (bottom) of the 20% perturbed input data ($M = 0.4, k_1 = 5.0$).

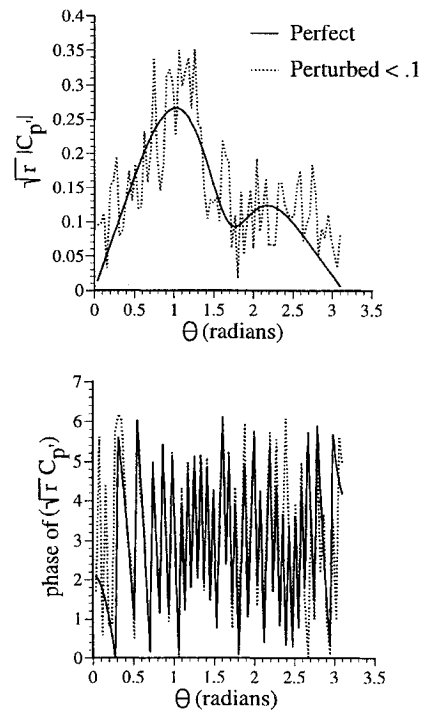

Fig. 6 Magnitude (top) and phase (bottom) of the uniformly perturbed (less than 0.1) input data ($M = 0.4, k_1 = 5.0$).

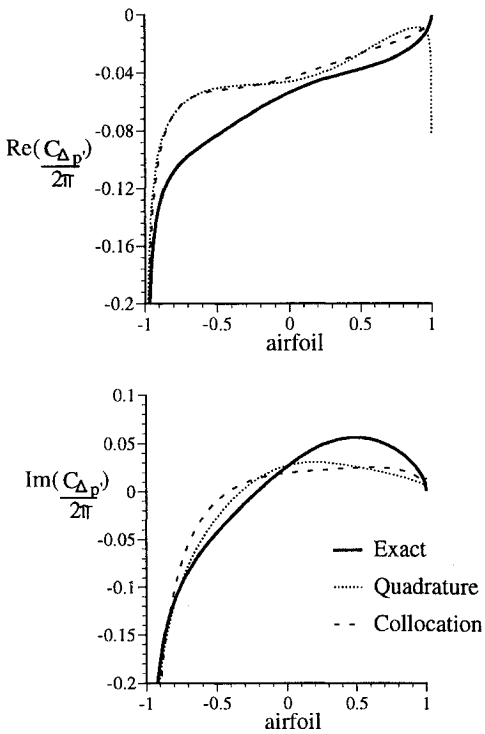

Fig. 5 Reconstruction with 20% perturbed input data: real (top) and imaginary (bottom) parts of the unsteady surface pressure ($M = 0.4, k_1 = 5.0$).

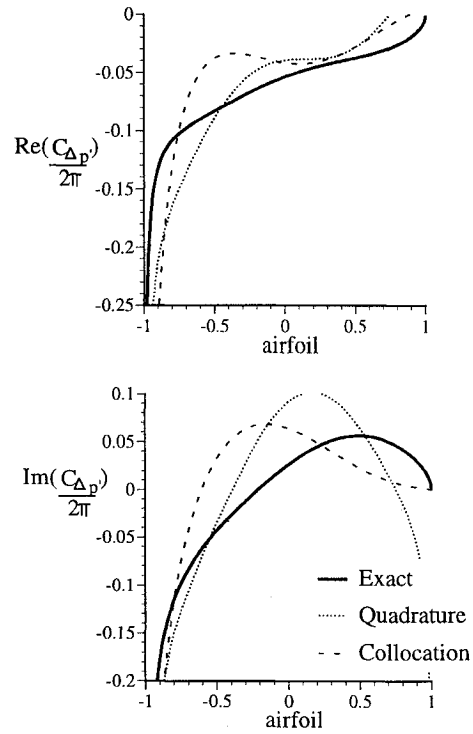

Fig. 7 Reconstruction with uniformly perturbed (less than 0.1) input data: real (top) and imaginary (bottom) parts of the unsteady surface pressure ($M = 0.4, k_1 = 5.0$).

Uniform Error

Rather than the error being a percentage of the data at a given location, often the error is more uniform at all locations. Thus we consider errors made by uniformly perturbing the data. In this case, random numbers less than or equal to 0.1 are added to or subtracted from the real and imaginary parts of the far-field data at every simulated measurement location. The perturbed input data are shown in Fig. 6. The reconstruction can be found in Fig. 7.

The reconstructions are less accurate than for the relative error case and can be improved. Such an improvement is obtained by eliminating the amplification of error in the data at measurement locations directly upstream and directly downstream of the flat-plate airfoil due to the division by $\sin\tilde{\theta}$ [see Eq. (23) in Part 1 (Ref. 1)]. Instead of using data locations on an arc from 0 to π, the arc is restricted from $\pi/8$ to $7\pi/8$. Using restricted input data yields a significant improvement in the reconstructions, as shown in Fig. 8. We also note that neglecting the measurements upstream and downstream in our simulation is consistent with experiments, since often a flow inlet and outlet are located directly upstream and downstream, respectively, and data will not be available from these regions.

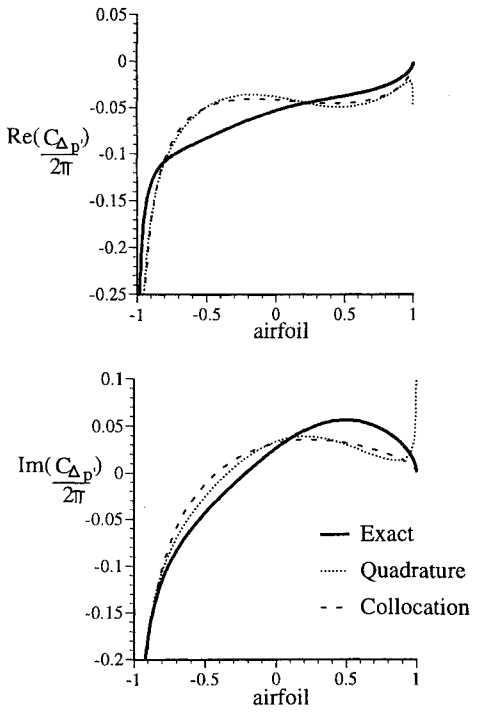

Fig. 8 Reconstruction with uniformly perturbed (less than 0.1) input data, neglecting upstream and downstream data: real (top) and imaginary (bottom) parts of the unsteady surface pressure ($M = 0.4, k_1 = 5.0$).

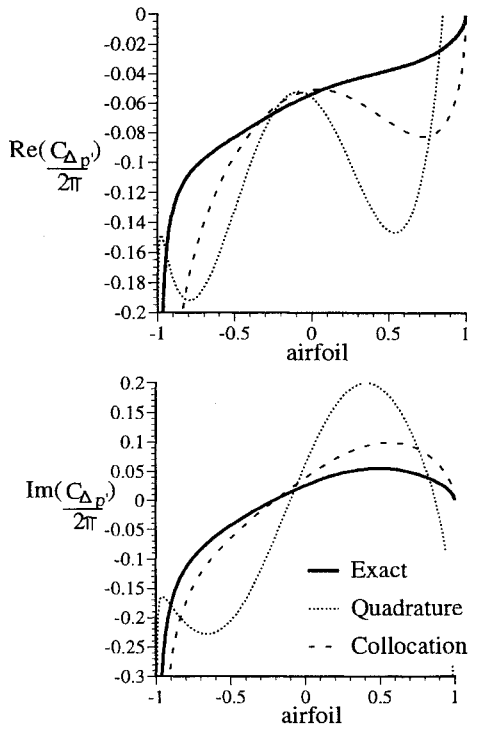

Fig. 10 Reconstruction with uniformly increased (0.05) input data: real (top) and imaginary (bottom) parts of the unsteady surface pressure ($M = 0.4, k_1 = 5.0$).

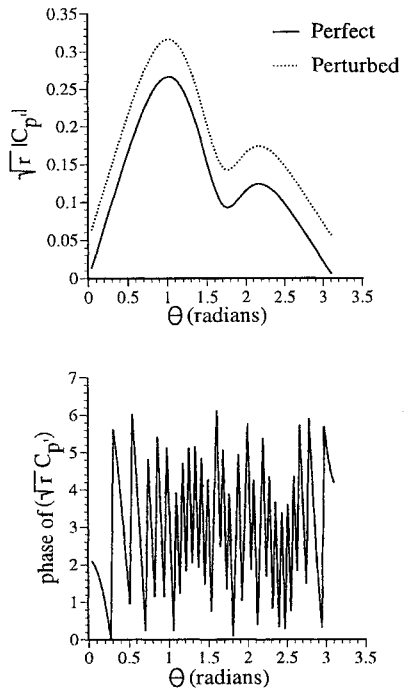

Fig. 9 Magnitude (top) and phase (bottom) of the input data when the magnitude is uniformly increased by 0.05 ($M = 0.4, k_1 = 5.0$).

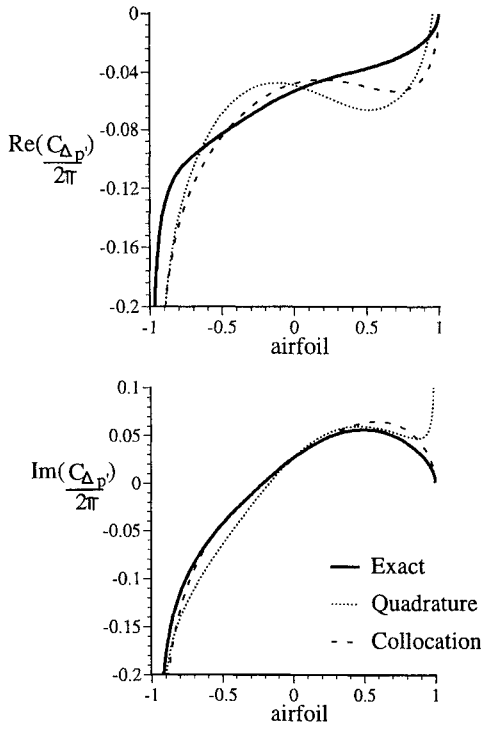

Fig. 11 Reconstruction with uniformly increased (0.05) input data, neglecting data upstream and downstream: real (top) and imaginary (bottom) parts of the unsteady surface pressure ($M = 0.4, k_1 = 5.0$).

General Bias

A general-bias error in the input data is the last type of error in the input data considered. Here the magnitude of the input data is increased by 0.05 everywhere as shown in Fig. 9. This type of error simulates a possible calibration bias in an experimental setup. The reconstructions seen in Fig. 10 are poor when all of the data are used. Again, removing the upstream and downstream data corresponding to $\theta = 0$ and $\theta = \pi$ significantly improves the reconstructions, as shown in Fig. 11.

Sensitivity to Frequency and Mach Number

The far-field pressure is not the only input for the inverse problem. Other inputs include k_1, k_3, and the Mach number. These parameters combine to give the value of

$$K = \sqrt{\frac{k_1^2 M^2}{\beta^4} - \frac{k_3^2}{\beta^2}}$$

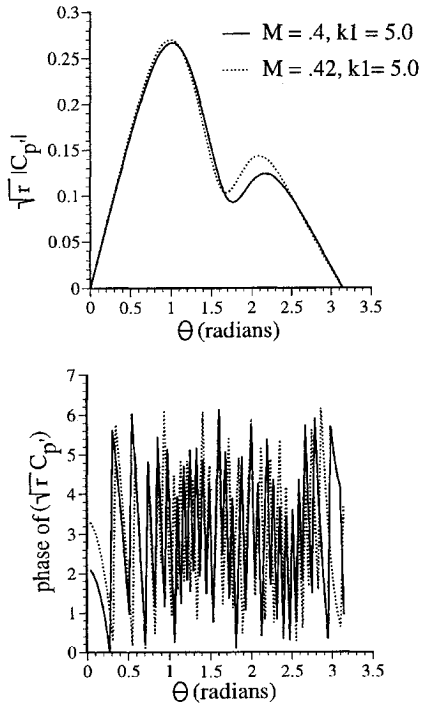

Fig. 12 Magnitude (top) and phase (bottom) of far-field data for $M = 0.4, k_1 = 5.0$ and $M = 0.42, k_1 = 5.0$.

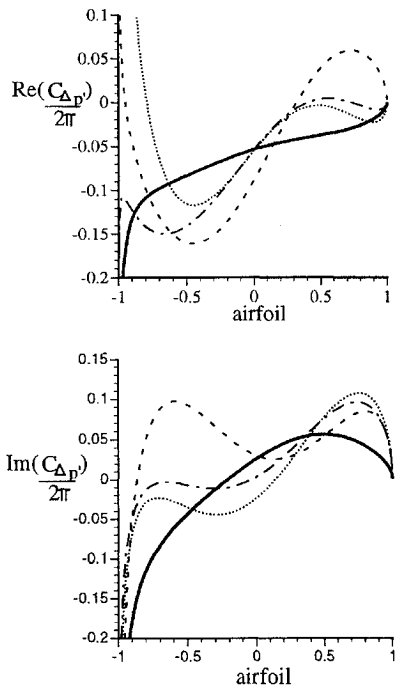

Fig. 13 Reconstruction using input parameters $M = 0.4, k_1 = 5.0$, but input data corresponding to $M = 0.42, k_1 = 5.0$ at $r = 100$, 10, and 5.0: real (top) and imaginary (bottom) parts of the unsteady surface pressure: ——, exact; · · · ·, collocation, $r = 100$; - - -, collocation, $r = 10$; and –·–, collocation, $r = 5$.

which defines the kernel. These parameters also arise in the transformation

$$P = p' e^{iMK_1\tilde{x}_1}$$

used to transform the governing equations into the Helmholtz equation.

The sensitivity of reconstructions to errors in these parameters is demonstrated using the case $M = 0.4, k_1 = 5.0$ and the collocation reconstruction method. The sensitivity is first demonstrated by

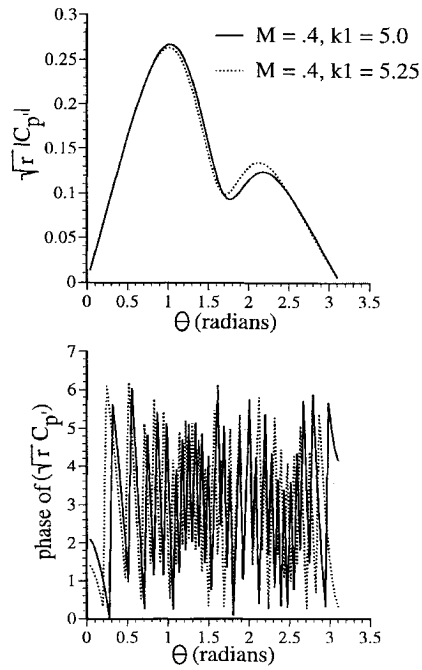

Fig. 14 Magnitude (top) and phase (bottom) of far-field data for $M = 0.4, k_1 = 5.0$ and $M = 0.4, k_1 = 5.25$.

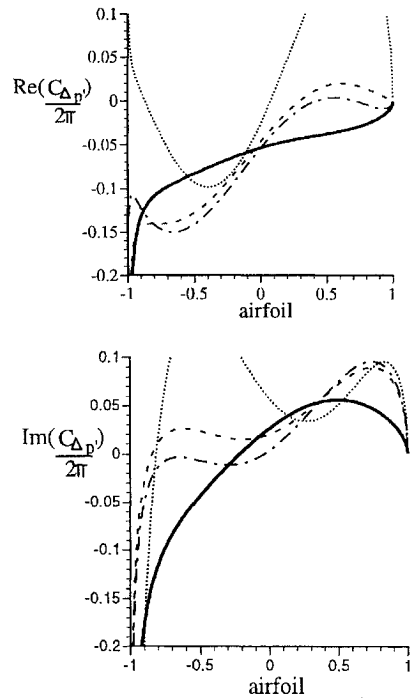

Fig. 15 Reconstruction using input parameters $M = 0.4, k_1 = 5.0$, but input data corresponding to $M = 0.4, k_1 = 5.25$ at $r = 100$, 10, and 5.0: real (top) and imaginary (bottom) parts of the unsteady surface pressure: ——, exact; · · · ·, collocation, $r = 100$; - - -, collocation, $r = 10$; and –·–, collocation, $r = 5$.

increasing the Mach number 5%. Figure 12 compares the far-field data for the cases $M = 0.4, k_1 = 5.0$ and $M = 0.42, k_1 = 5.0$. The reconstruction found from the collocation method with the input data corresponding to $M = 0.42, k_1 = 5.0$ but input parameters of $M = 0.4, k_1 = 5.0$ is plotted as the dotted line in Fig. 13. No improvement is seen when the regularization method or regularization parameter is changed, or when the data directly upstream and downstream of the airfoil are neglected.

In a second example, the reduced frequency is increased by 5%. Figure 14 compares the far-field data for the cases $M = 0.4, k_1 = 5.0$

and $M = 0.4, k_1 = 5.25$. The reconstruction determined from input data corresponding to $k_1 = 5.25$ but input parameter $k_1 = 5.0$ is represented by the dotted line in Fig. 15. Again, the reconstruction is not accurate, and changes in the regularization or data locations do not improve it.

At large distances, the asymptotic form of the kernel includes the term $e^{iK\tilde{r}}$, where K is a function of Mach number and reduced frequency. Therefore, when $\tilde{r}$ is very large, any error in K is significantly amplified. This suggests reducing $\tilde{r}$ by using measurements in the far field. For example, we take r to be on the order of 10 rather than 100, as in the preceding tests. The reconstructions obtained when $r = 10$ and $r = 5$ in the preceding two examples are shown in Figs. 13 and 15. Some improvement can be seen. In other test cases, errors in the input parameters on the order of 1% are completely tolerated when the input data are taken at $r = 10$. Errors larger than 1%, however, do alter the reconstructions even when the input are taken at a distance of $r < 10$. In summary, the inverse aeroacoustic problem is much more sensitive to errors in the input parameters than to errors in the input data.

Conclusion

In Part 1, methods for the aeroacoustic inversion were developed that yield very accurate reconstructions of the unsteady pressure on a flat-plate airfoil when "perfect" far-field input are available. The "perfect" input data for testing the schemes are generated numerically by solving the direct problem. The test with "perfect" input data and accurate input parameters established the theoretical feasibility of the inversion. In the current paper, we address the practical aspect of the inverse problem by considering imperfect input data.

In practice, when the far-field input data are obtained experimentally, they will contain some noise. Therefore, various sensitivity analyses are implemented to demonstrate the practical feasibility of the reconstruction. By adding noise to the input data through three different methods, our analyses show sensitivity of the inverse solutions to error in the input data. To assess the impact of these errors on the inverse problem, we have considered three types of errors: relative, uniform, and bias. The results show that the sensitivity of the inverse solution to errors in the input data can be controlled by an optimal choice of the regularization and by disregarding input data located directly upstream and downstream of the airfoil.

A similar sensitivity analysis of the effect of mean-flow parameters—Mach number and reduced frequency—shows that this sensitivity is not as easily controlled. Errors in these parameters affect the kernel of the integral equation directly, which in turn affects the matrix. Altering the regularization parameter and neglecting some of the data do not improve the reconstructions. It is shown, however, that the use of midfield data produces a significant improvement in the reconstructions. Note that this idea must be implemented using the general form of the kernel because the input data will be taken in the midfield or near field. This precludes using the schemes with the expanded form of the kernel.

Acknowledgments

The research was supported by U.S. Office of Naval Research Grant N00014-92-J-1165 and monitored by L. Patrick Purtell. Sheryl M. Grace would like to thank Zonta International and The Center for Applied Mathematics at the University of Notre Dame for their support.

References

[1]Patrick Grace, S., Atassi, H. M., and Blake, W. K., "Inverse Aeroacoustic Problem for a Streamlined Body Part 1: Basic Formulation," *AIAA Journal* Vol. 34, No. 11, 1996, pp. 2233–2240.

[2]Atassi, H. M., Dusey, M., and Davis, C. M., "Acoustic Radiation from a Thin Airfoil in Nonuniform Subsonic Flow," *AIAA Journal*, Vol. 31, No. 1, 1993, pp. 12–19.